An action-observation network in the common marmoset identified by ultra-high field fMRI

Alessandro Zanini[1,*], Audrey Dureux[1], Stefan Everling[1,2,*]

Author affiliations:

[1]Centre for Functional and Metabolic Mapping, Robarts Research Institute, University of Western Ontario, London, Ontario, Canada

[2]Department of Physiology and Pharmacology, University of Western Ontario, London, Ontario, Canada

*Corresponding authors:

Alessandro Zanini, Robarts Research Institute, University of Western Ontario, London, Ontario, Canada. **Email**: azanini4@uwo.ca

Stefan Everling, Robarts Research Institute, University of Western Ontario, London, Ontario, Canada**. Email:** severlin@uwo.ca

Abstract

Thirty years have passed since the first description of neurons in Old World macaque monkeys that fire both during the execution and observation of goal-directed actions. Since then, these so-called "mirror neurons" have been shown to play important roles in understanding the actions of others, learning by imitation, and social cognition in macaques and humans. In contrast to Old World primates, an action-observation network has not yet been identified in New World primates. Here we used ultra-high field fMRI at 9.4T in awake common marmosets (*Callithrix jacchus*) while they watched videos depicting the upper-limb of marmosets performing goal-directed (grasping food) or non-goal-directed actions. We found that the observation of goal-directed actions, compared to non-goal directed ones, activated a frontotemporoparietal network, including areas 6 and 45 in premotor and prefrontal cortices, and areas PGa-IPa, FST, and the TE complex in temporoparietal regions. These results demonstrate the existence of an evolutionarily conserved action observation network in primates that likely predates the separation of Old and New World monkeys.

Keywords

Marmoset, mirror neurons, action observation network, fMRI, grasping

Introduction

Thirty years have passed since the first unexpected finding of neurons in Old World macaque monkeys that were active not only during the execution of goal-directed actions, but also during their observation (di Pellegrino et al., 1992). This ability to “reflect” others’ actions earned them the name "mirror neurons" (Gallese et al., 1996; Rizzolatti et al., 1996) and made them one of the most striking discoveries in the field of cognitive neuroscience. Mirror neurons likely play important roles in understanding the actions of others, learning by observation (Ramsey et al., 2021), imitation (Iacoboni et al., 1999), and in motor rehabilitation (Nogueira et al., 2021; Rizzolatti et al., 2021). Furthermore, the mirror neuron system (MNS) is also strongly involved in multiple facets of social cognition, such as empathy or emotional contagion (Bekkali et al., 2021; Paz et al., 2022) and its malfunction has been reported in several neurodegenerative pathologies (Farina et al., 2020) and in autism spectrum disorders (Yates & Hobson, 2020).

The first electrophysiological studies in macaques found mirror neurons in the dorsal part of premotor area F5 (di Pellegrino et al., 1992; Gallese et al., 1996; Rizzolatti et al., 1996). A fundamental factor for the activation of these neurons was the purpose of the act: observation of a grasping movement only activated these neurons if the grasp was performed to an object (goal-directed action) and not an empty space (non-goal-directed action). Rizzolatti's group interpreted this mirroring mechanism as a neural correlate for mapping the actions of others to one's own repertoire of motor acts, for imitation or understanding purposes. This view is strengthened by the fact that the observation of the initial part of the movement and the knowledge about the existence of a hidden target is sufficient to induce the response (Umiltà et al., 2001). The complete motor representation of the observed action can thus be internally generated, thanks to the activity of the MNS. Subsequently, Ferrari and colleagues observed populations of neurons in the ventral part of area F5 capable of reproducing mirror-type responses for actions carried out with the mouth (i.e., grasping, sucking), revealing a first somatotopic organization of the MNS (Ferrari et al., 2003).

Outside of premotor cortex, neurons activated during the observation of others’ actions have been found in the macaque superior temporal sulcus (STS) (Perrett et al., 1989). One hypothesis is that the STS provides the essential visual input to the MNS in order to map others’ actions in our own repertoire (Nelissen et al., 2011), but that communication between this temporal region and the frontal areas can only take place through connections with the rostral part of the inferior parietal lobule (Matelli et al., 1986; Petrides & Pandya, 1984) and the anterior intraparietal

area (AIP, Nelissen et al., 2011). This hypothesis is supported by the discovery of populations of mirror neurons in parietal areas PF and PFG in macaques that respond in an action goal-related manner, with different activity if the same movement is carried out (or observed) with different behavioural goals (i.e., grasping food to bring it to the mouth or to place it in a container, Fogassi et al., 2005; Fogassi & Luppino, 2005; Gallese et al., 2002). Neurons with mirror-like response properties have also been observed in the dorsal premotor (PMd) and motor (M1) cortices of macaques (Cisek & Kalaska, 2004; Dushanova & Donoghue, 2010; Tkach et al., 2007). However, the responses of these neurons during the observation of actions seem to be conditioned by the previous training in the execution of those same movements.

A confirmation for these electrophysiological findings has come from fMRI studies in macaques, in which the viewing of videos depicting goal-directed actions was associated with activations in premotor area F5 and in prefrontal area 45 (Nelissen et al., 2005; Sliwa & Freiwald, 2017), in parietal cortex and in the STS (Sliwa & Freiwald, 2017).

In humans, numerous fMRI studies have found regions homologous to those described in macaque monkeys, such as the ventral premotor cortex and the posterior regions of the inferior frontal gyrus (putative human homologue of area F5, Aziz-Zadeh et al., 2006; Buccino et al., 2004; Ferri et al., 2015; Kilner et al., 2009), the inferior parietal lobule (IPL, Arnstein et al., 2011; Chong et al., 2008; Iacoboni et al., 1999; Rizzolatti et al., 2001; Rizzolatti & Craighero, 2004) and the STS (Grèzes et al., 2003; Saxe et al., 2004). In addition to these "classical" regions, mirror responses have also been identified at the level of the motor (Fadiga et al., 2005) and the premotor dorsal cortices (Grèzes et al., 2003) and subcortically, in the hippocampus (Mukamel et al., 2010). Molenberghs and colleagues' meta-analysis confirmed this widespread network, adding to the human MNS portions of the middle and inferior temporal gyrus, of the cingulate gyrus, the cerebellum, and the primary visual cortex (Molenberghs et al., 2012).

Support for a putative MNS in New World monkeys has come from an electrophysiological study by Suzuki and colleagues, who recorded from a small number of mirror neurons in the ventrolateral frontal region and in the STS of the common marmoset (*Callithrix jacchus*) (Suzuki et al., 2015). This small New World primate lives in family groups and shares important social similarities with humans, such as prosocial behavior, imitation, and cooperative breeding. Their small size combined with recent wireless and datalogger recording techniques additionally make it possible to record high density neural activity during natural social behaviour in this species.

Their lissencephalic (smooth) cortex offers the opportunity for laminar electrophysiological recordings and optical imaging in many cortical areas. All of these features could make marmosets an excellent primate model for the study of the neural basis of action observation.

To identify a putative action observation network in marmosets, we employed whole-brain ultra-high-field awake fMRI at 9.4T. Similar to previous macaque studies (Nelissen et al., 2005, 2011), we investigated the activations induced by the presentation of videos representing the upper limb of a marmoset performing a goal-directed (reaching and grasping for food) or non-goal-directed movement (reaching and grasping to an empty space).

Results

In this fMRI study we used a block-design in which each run contained 8 video sequences belonging to four different experimental conditions, alternating with baseline blocks. The videos belonging to the Grasping Hand condition showed the upper limb of a marmoset performing a complete reaching and grasping movement of a small piece of food (i.e., a small marshmallow). In the Empty Hand condition, a similar movement was shown, but in this case the piece of food was absent, rendering the action non-goal-directed. The last two experimental conditions (Scrambled Grasping Hand and Scrambled Empty Hand) were the phase-scrambled version of these two classes of videos (see Methods section for details). Four common marmosets were included in the study, using ten runs per animal in the analyses (40 runs in total).

Occipito-temporal activations induced by condition-specific movies

We first compared the activations in the four experimental conditions versus the baseline blocks (one sample t-test, cluster-defining threshold $p<0.001$ and $\alpha=0.05$ for all contrasts). Figure 1 shows the group maps on fiducial brain surfaces (left hemisphere, see Supplementary Figure S1 for the right hemisphere) using the Paxinos parcellation of the NIH marmoset brain atlas (Liu et al., 2018). Common activations (see Supplementary Table T1 for complete report) include large portions of the occipital lobe, with a bilateral cluster covering V1, V2, V3, V3A, V4, V4T, V5 (MT), V6, and area 19. These strong visual responses allowed us to further verify that marmosets were visually engaged in the task. Further activations common to all experimental conditions were found in the temporal lobe, both at the border with the parietal cortex (medial superior temporal area, or MST, and fundus of superior temporal sulcus, or FST) and more ventrally, including different portions of the TE complex (areas TE3, TE occipital part) and the fundus of the superior temporal ventral area (the more ventral part of parietal areas PGa and IPa) bilaterally. However, temporal activations were stronger and more extended in the Grasping and Empty Hand conditions, as illustrated in Figure 1A and 1B, including the bilateral temporo-parieto-occipital association area (TPO). Finally, the Grasping Hand condition showed activations in the TE complex (TE1 and T1, bilaterally) and in area 36. Regarding the ventral region of the temporal lobe, all conditions showed activations in the occipital portions of the right temporal areas TL and TH. The Grasping Hand and both the scrambled conditions further showed activations in the occipital portion of right area TF (TFO). The largest cluster of activation in this region is observed in the Grasping Hand

condition, including right area TF and extending the above-described activations to the left hemisphere.

Additional differences between the phase-scrambled conditions and those showing an "intact" movement were present in the posterior parietal cortex (PPC). Both the Grasping and Empty Hand conditions showed extensive and bilateral activations in the intraparietal areas (MIP, LIP, VIP) and in area PG. These activations are partly present, although weaker, in the Scrambled Grasping Hand condition. The Grasping movement also seems to preferentially activate bilaterally area PE and its caudal portion (PEC), but also bilaterally the anterior intraparietal area (AIP). The observed parietal activation cluster ends with the translational occipito-parietal area (Opt) in all tested conditions.

The clearest differences observed were present in premotor and prefrontal cortex. Only the goal-directed action in the Grasping Hand condition induced a strong activation of bilateral prefrontal and premotor areas, with a cluster including the rostral and caudal portions of the dorsal premotor cortex (6DR and 6DC), the ventral premotor cortex (6Va) and the left supplementary motor cortex (6M). In the dorsolateral prefrontal cortex (dlPFC) we observed bilateral activations of area 8 (8C and 8aV, plus left 8b and 8aD). This prefrontal cluster continued into areas 47 (lateral, medial and orbital portions) and 45 in the ventrolateral prefrontal cortex (vlPFC), area 24 (24a and 24b) in the medial prefrontal cortex (mPFC) and areas 11 and 13 (13a, 13b and 13M) in the orbitofrontal cortex (OFC), bilaterally. This type of activation is in line with previous findings in macaque monkeys (di Pellegrino et al., 1992; Gallese et al., 1996; Nelissen et al., 2005; Rizzolatti et al., 1996).

At the subcortical level, activations common to all the experimental conditions were present in the bilateral anterior ventral nucleus of the thalamus, the pulvinar, in the parahippocampal formation (in both cases the involvement seems to include the most dorsal and posterior portions), and in the lateral geniculate nucleus. In addition, the Grasping Hand condition was also associated with activations in the medial geniculate nucleus, amygdala and septum.

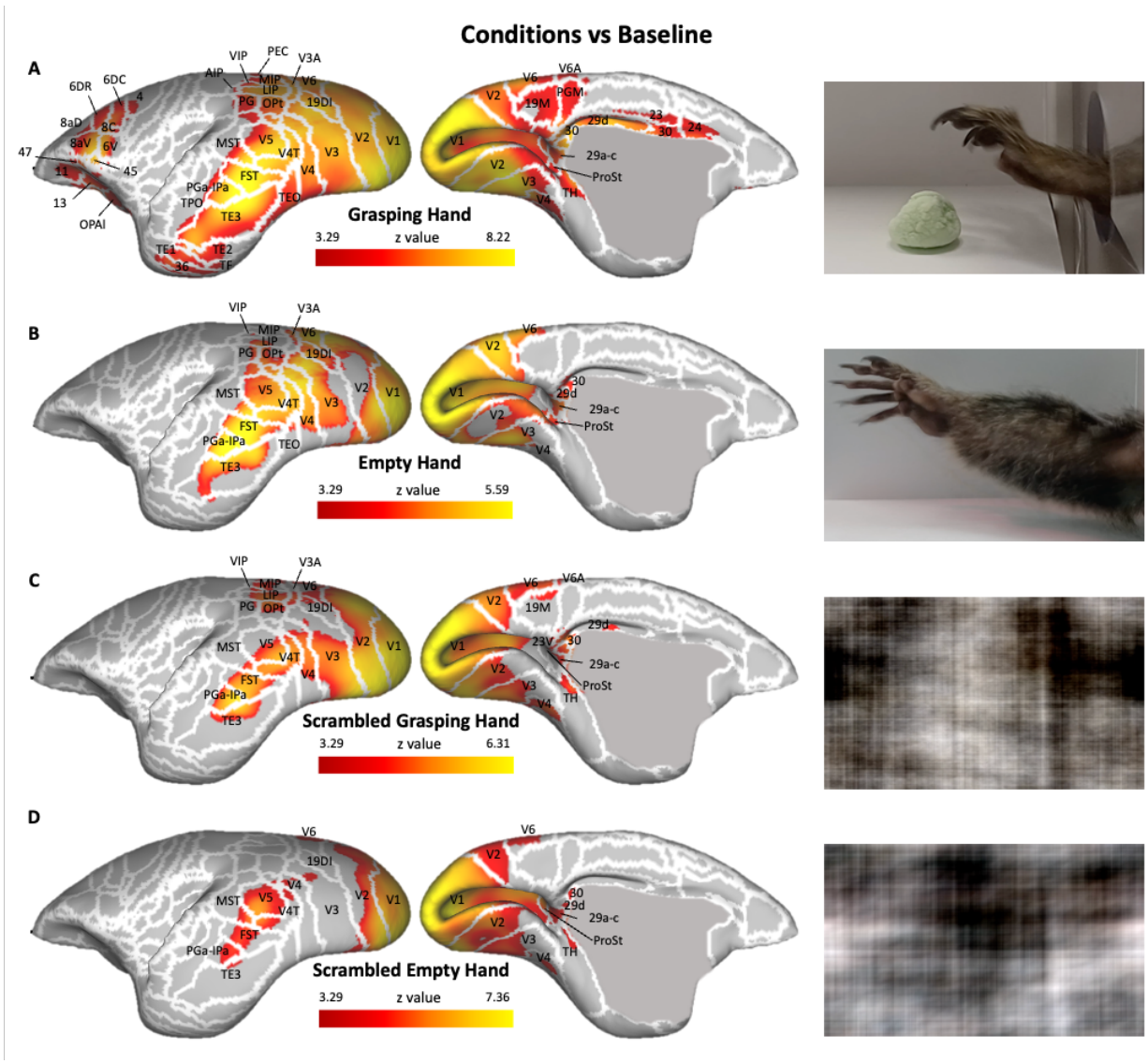

Figure 1. Functional maps of the contrasts between each condition and baseline. Grasping Hand (A), Empty Hand (B), Scrambled Grasping Hand (C) and Scrambled Empty Hand (D) maps are displayed on the left fiducial brain surface (lateral view on the left, medial view on the right). White lines delineate the cerebral areas included in the Paxinos parcellation of the NIH marmoset brain atlas (Liu et al., 2018). The responses here reported have intensity higher than z = 3.29 (corresponding to $p<0.001$, AFNI's 3dttest++) and survived the cluster-size correction (10000 Monte-Carlo simulations, with $\alpha=0.05$).

A fronto-temporal network to process vision of body-parts in motion

We next performed an analysis to identify brain activations induced by videos displaying intact movements (i.e, a movement of an arm and hand), without considering the goal of the action, (Grasping and Empty Hand conditions), versus phase-scrambled videos of these movements (Scrambled Grasping and Empty Hand conditions). The results of this group-level analysis are shown in Figure 2 (paired t-test, results reported at $p<0.001$ and corrected for cluster-size threshold

via Monte Carlo simulations, with α=0.05). We found that the observation of the intact movement videos elicited stronger activations both in the occipital (in high-level visual areas, such as V4, V4T and V6) and temporal cortex. In the latter case, we observed two large bilateral activation clusters, including area FST, the PGa-IPa conjunction, wide portions of the TE complex (TE1, TE2, TE3 and TEO) but also more ventral regions, such as area 36. In the right hemisphere, this contrast revealed activation peaks also in the medial superior temporal area (MST) and in MIP.

These results show regions activated by videos of grasping movements with or without goal-directed actions, consistent with previously described body patches in the marmoset temporal cortex (Hori et al., 2021; Hung et al., 2015).

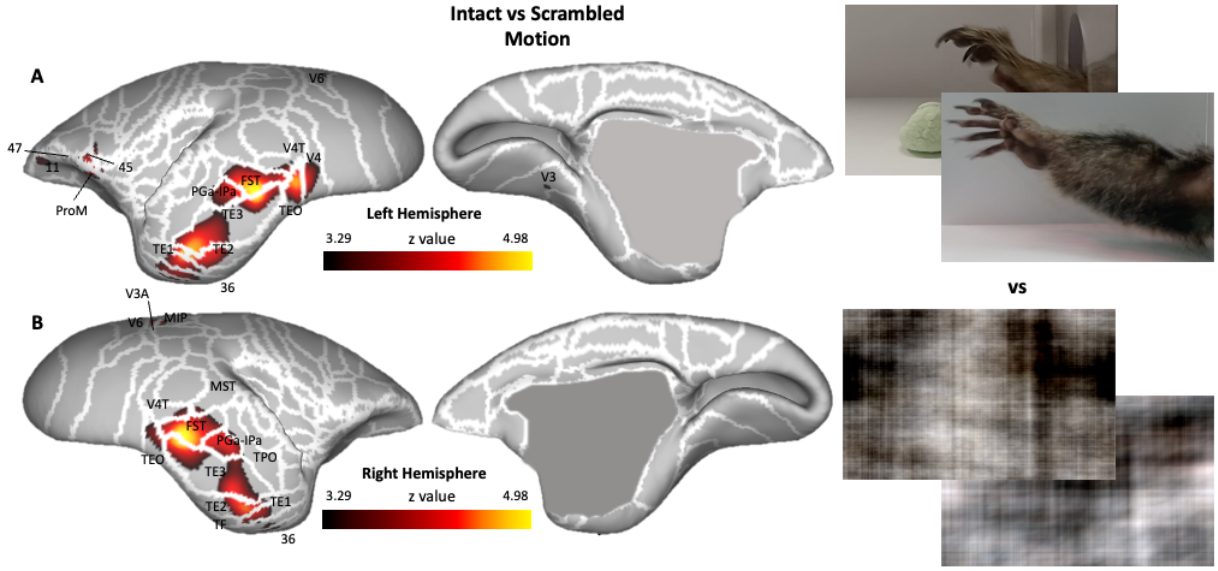

Figure 2. Functional maps of the contrasts between the "Intact" versus the "Scrambled" Motion conditions. Maps are displayed on the left (A) and right (B) fiducial brain surfaces (lateral view on the left, medial view on the right). White lines delineate the cerebral areas included in the Paxinos parcellation of the NIH marmoset brain atlas (Liu et al., 2018). The responses here reported have intensity higher than z = 3.29 (corresponding to p<0.001, AFNI's 3dttest++) and survived the cluster-size correction (10000 Monte-Carlo simulations, α=0.05).

An action-observation network for goal-directed actions

One of the defining features of mirror neurons is that they discharge at higher rates for goal-directed than non-goal-directed actions (di Pellegrino et al., 1992; Gallese et al., 1996; Rizzolatti et al., 1996). To test whether areas in the marmoset brain show a similar pattern, we compared the activations elicited by the Grasping conditions with the Empty Hand conditions (paired t-test, results reported at p <0.001 with cluster-size threshold determined by Monte Carlo simulations for

α=0.05). The results show a large network of frontotemporoparietal regions that is significantly stronger activated in the Grasping condition compared to the Empty Hand condition (Figure 3). The premotor cluster includes the rostral and caudal dorsal premotor cortices (6DR and 6DC) and the ventral premotor cortex (6Va), bilaterally. These clusters extend to a small portion of dlPFC (8C, 8aV) and to the vlPFC (45, 47 medial and lateral). The bilateral OFC (11, 13) and the left mPFC (24, 32) showed the same pattern. A similar bilateral response cluster is found at the temporal level, where the observation of a goal-directed action induced stronger responses in the FST, in the PGa-IPa junction and in the inferior temporal area (TE1, TE2 and TE3).

A bilateral cluster of preferential activation for goal-directed actions is also present in the occipital cortex, with some differences between the two hemispheres: while in the left hemisphere the most extensive activation is found in the region between V2 (lateral and ventral portions) and V3 (dorsal) and in the ventro-medial part of V2, in the right hemisphere this cluster seems to include more higher-level areas, covering the region between V3 (the more dorsal portion), V4, V4T and MT (V5).

In addition to these bilateral activations, we also observed unilateral activations. In the left hemisphere, the intraparietal area (LIP) was activated, while in the right hemisphere activations were observed in the posterior cingulate region, corresponding to medial areas 29 and 30. Subcortically, we found activations in the hippocampal formation (right hemisphere) and in the thalamus (bilaterally), with a cluster that extended into the border region between the medial and lateral portion of the anterior ventral nucleus, and a second more posterior cluster in the pulvinar.

These results strongly support the existence of a widespread frontotemporoparietal network activated by the observation of goal-directed reaching and grasping movements, similar to the MNS in humans and macaque monkeys (see Casile, 2013; and Rizzolatti & Craighero, 2004 for review).

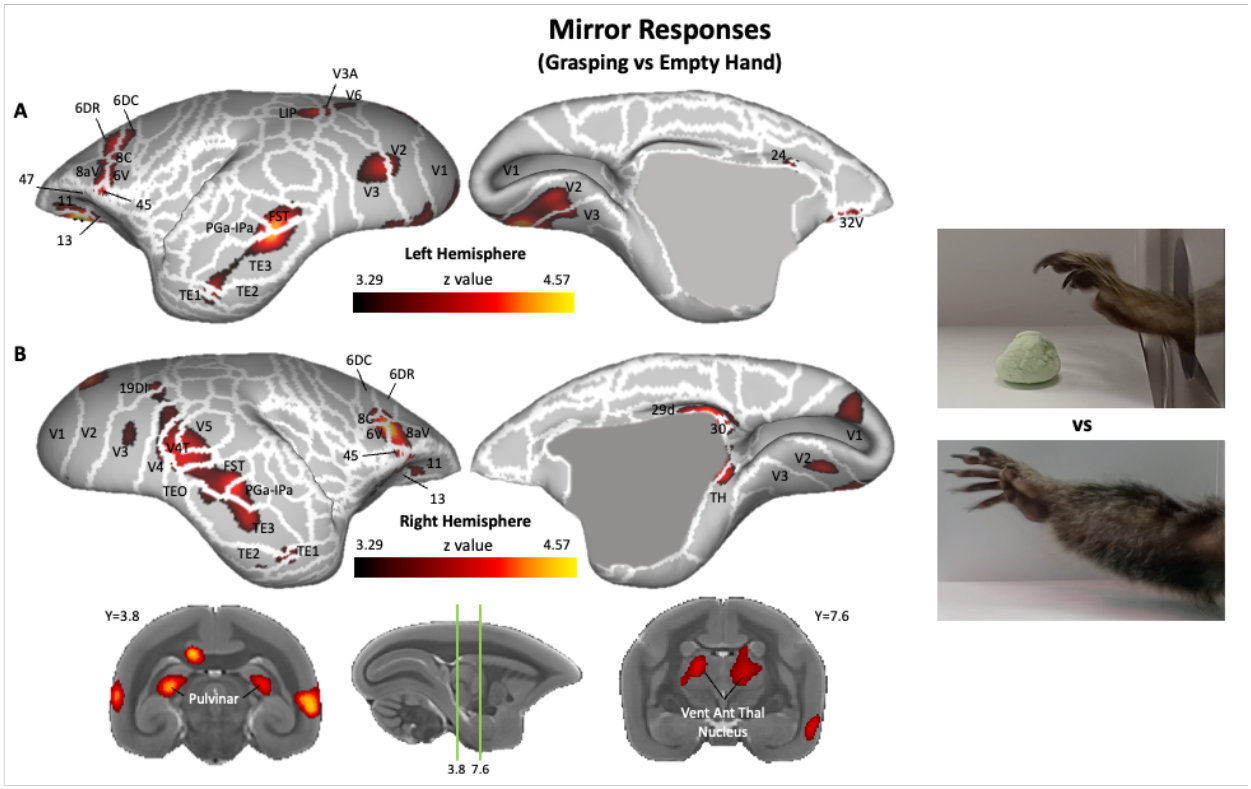

Figure 3. Functional maps of the contrasts between Grasping Hand and Empty Hand conditions. Maps are displayed on the left (A) and right (B) fiducial brain surfaces (lateral view on the left, medial view on the right). White lines delineate the cerebral areas included in the Paxinos parcellation of the NIH marmoset brain atlas (Liu et al., 2018). The responses here reported have intensity higher than z = 3.29 (corresponding to p<0.001, AFNI's 3dttest++) and survived the cluster-size correction (10000 Monte-Carlo simulations, α=0.05).

ROI-based time series comparisons

We extracted the time series from ROIs of selected areas found in the literature to be part of the MNS in humans and macaques (6Va, 6Vb, 45, FST, PG and PFG, all bilaterally) and compared the magnitude of the responses in the different experimental conditions (see Figure 4) through paired t-tests corrected for multiple comparisons (FDR correction). Three ROIs showed stronger responses in the case of goal-directed actions (Grasping_Hand) compared to both non-goal-directed actions (Empty_Hand, 45: $t_{(39)}$=5.32 p<0.001; FST: $t_{(39)}$=4.52 p<0.001; 6Va: $t_{(39)}$=2.38 p=0.04) and to its phase-scrambled version (Scrambled_Grasping_Hand, 45: $t_{(39)}$=6.13 p<0.001; FST: $t_{(39)}$=5.63 p<0.001; 6Va: $t_{(39)}$=2.80 p=0.02). A fourth region showing the same response pattern is parietal area PG, but the results from the t-tests where not significant following corrections for multiple comparisons (Grasping_Hand vs Empty_Hand: $t_{(39)}$=2.48 p=0.06; Grasping_Hand vs Scrambled_Grasping_Hand: $t_{(39)}$=2.23 p=0.06). We only found a significant

difference between the Empty_Hand condition and its phase-scrambled version ($t_{(39)}$=2.38 p=0.03) in the FST ROI.

The only experimental condition showing a significant difference from zero (considered as baseline) in all the ROIs investigated is the one depicting a goal-directed action (in all cases, corrected p<0.05 or more). This supports a greater involvement of these areas when observing others' actions, specifically when these are directed towards an object.

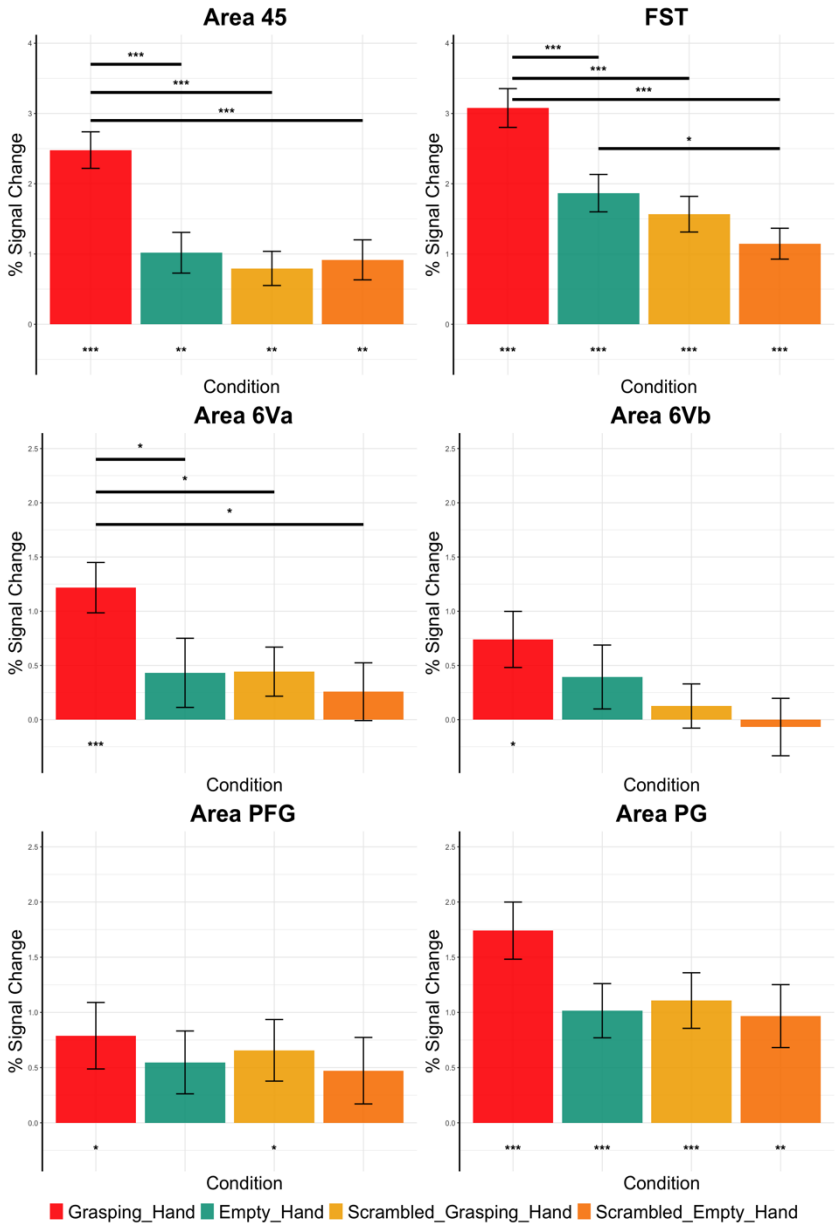

Figure 4. Magnitude of the difference in the responses between conditions within 6 ROIs. Using the Paxinos parcellation of the NIH atlas (Liu et al., 2018), we created six bilateral regions of interest, from which we extracted the time series per condition. Differences between conditions (horizontal bar and asterisks) and from the baseline (asterisks below each graph column) were tested through paired t tests corrected for multiple comparisons (FDR). Error bars represent the standard error from the mean. Asterisks represent p<0.05 (*), p<0.01 (**) and p<0.001 (***).

Discussion

Observing and understanding others' actions is crucial for social animals like primates. Numerous studies have shown that a frontotemporoparietal network mediates this function in Old World macaques and humans. This so-called mirror neuron system (MNS) responds in particular to goal-directed actions (Gallese et al., 1996; Rizzolatti et al., 1996), e.g. grasping of an object. In this study, we investigated the existence of an action-observation networking in the common marmoset, a small New World primate that is becoming popular as powerful additional nonhuman primate model (Okano, 2021). For this purpose, we presented 4 awake marmosets with videos depicting a finalized action (grasping food) or a similar but non-goal-directed action (grasping air) in an fMRI block-designed task, alternated by videos of their phase-scrambled versions.

The comparison between videos depicting an action ("intact") and their phase-scrambled versions elicited strong activations in the occipital and temporal lobes, consistent with what we observed in previous studies (Cléry et al., 2021; Schaeffer et al., 2020) and overlapping with the location of body and face neural patches (Hori et al., 2021; Hung et al., 2015). These activations, proceeding in the caudo-rostral direction, include portions of areas V4/ V4T, TEO, FST and PG. More ventrally, a second temporal cluster overlaps with areas TE and 36. These patches therefore seem to respond specifically to the presentation of a part of the body (the hand or the entire arm). Furthermore, we observed activations in areas 45 and 47 in the left prefrontal cortex. We have found a similar activation following the presentation of videos of marmosets faces (Schaeffer et al., 2020) or marmosets carrying out social/non-social actions (Cléry et al., 2021). The results of the present study broaden the interpretations regarding this frontal patch, as the region located at the junction between areas 45 and 47 does not seem to be linked specifically to the processing of faces, but also to parts of the body in movement.

The main finding of this study comes from the comparison between goal-directed and non-goal-directed actions. As already observed by the first electrophysiological (di Pellegrino et al., 1992; Gallese et al., 1996; Rizzolatti et al., 1996) and neuroimaging studies (Nelissen et al., 2005, 2011) in macaques, neurons in the MNS show greater activity during the observation of goal- versus non-goal-directed movements. It has been hypothesized that this feature could provide the basis of the ability to recognize others' actions and understand their behavior and intentions (Umiltà et al., 2001).

While the existence of a MNS has been established in both human (see Molenberghs et al., 2012 for a meta-analysis) and non-human Old World primates (see Casile, 2013 for review), only a small number of mirror neurons have been identified in the ventrolateral frontal region of New World marmosets (Suzuki et al., 2015). Our study represents the first support for a putative MNS in the common marmoset. This network in marmosets shows strong correspondences with the MNS in macaques and humans. The first mirror neurons in macaques have been observed in areas F5 and 45 (di Pellegrino et al., 1992; Gallese et al., 1996; Nelissen et al., 2005; Rizzolatti et al., 1996), and regions with similar properties have also been found with fMRI in homologous brain areas in humans (Aziz-Zadeh et al., 2006; Buccino et al., 2004; Ferri et al., 2015; Kilner et al., 2009). Our results show that large parts of the bilateral marmoset area 6V (likely corresponding to macaque's area F5 and human area PMv) and of the ventrolateral prefrontal cortex (areas 45, 47 and 13 bilaterally) are part of this putative MNS network. These findings are also in line with single neuron recordings in marmosets (Suzuki et al., 2015). The homologies between the MNS of the three species continue with activations in the dorsal area 6 (6DR and 6DC, bilaterally), mirroring what has been observed by electrophysiological (Cisek & Kalaska, 2004; Tkach et al., 2007) and fMRI studies (Grèzes et al., 2003) in macaques and humans, respectively.

Outside the premotor and prefrontal cortex, one of the main MNS regions is the STS, in both humans (Grèzes et al., 2003; Saxe et al., 2004) and macaques (Nelissen et al., 2011; Perrett et al., 1989). In the present study, we also found a posterior region in the fundus of the temporal sulcus (FST) in the New World marmoset that was more active for the observation of goal-directed versus non-goal-directed movements, consistent with the findings of a macaque fMRI study that used a similar experimental paradigm (Nelissen et al., 2011). In marmosets, this cluster extends also towards more lateral and inferior temporal regions, involving the ventral part of the FST (PGa-IPa area) and the more dorsal part of area TE3. Despite the presence of a preferential response during the observation of goal-directed actions, this temporal region is not usually included in the network of mirror neurons, as it does not encode motor-related activity (Molenberghs et al., 2012; Rizzolatti & Craighero, 2004). In marmosets, there is evidence of a small number of neurons that respond both when performing and observing grasping actions, but the activity was much lower in the execution condition (Suzuki et al., 2015). The absence of a motor execution component in our paradigm, however, does not allow us to determine whether any of the identified regions is also involved in motor execution. Interestingly, we also found a small region activated by the

observation of goal-directed actions more ventrally in the temporal lobe, at the junction between the TE1 and TE2 areas, bilaterally. At the moment, there is no evidence regarding the involvement of these ventral temporal areas in the MNS of humans or macaques. However, similar activation clusters have been reported by fMRI studies in marmosets using pictures of marmoset faces or body parts (Hori et al., 2021; Hung et al., 2015), videos of faces in different perspectives (Schaeffer et al., 2020), and videos of marmosets performing social or non-social goal-directed actions (Cléry et al., 2021). It is therefore conceivable that these regions are not strictly related to the MNS, but may be involved in the processing of faces and body parts of conspecifics. Further studies focusing on these temporal areas are needed in order to elucidate their function in these experimental settings.

Surprisingly, our study did not identify mirror-responses at the level of the inferior parietal lobule, one of the hubs of the MNS often reported in human (Arnstein et al., 2011; Chong et al., 2008; Iacoboni et al., 1999; Rizzolatti et al., 2001; Rizzolatti & Craighero, 2004) and macaque studies (Fogassi et al., 2005; Fogassi & Luppino, 2005; Gallese et al., 2002; Rizzolatti & Craighero, 2004; Rozzi et al., 2008). The rostral part of the inferior parietal lobule (IPL) would indeed be the MNS junction between the visual input coming from the STS and directed to the prefrontal and premotor cortices, structures not directly connected to each other in the macaque monkey (Matelli et al., 1986; Petrides & Pandya, 1984; Seltzer & Pandya, 1989). Conversely, recent studies demonstrated a direct bidirectional connection between the ventrolateral prefrontal cortex, including area 6V, and the FST in common marmosets (Burman et al., 2015; Suzuki et al., 2015). This could explain the lower parietal response reported in our study compared to the observation of goal-directed actions. However, the analysis of the time series showed a preference (albeit only marginally significant) of the inferior parietal area PG for videos depicting goal-directed actions, compared to all other experimental conditions. The role of this region is still largely unknown, but area PG has been identified as an important cortical hub in the common marmoset (Ghahremani et al., 2017; Theodoni et al., 2022), being involved in several different networks. It is therefore conceivable that this region is involved in the MNS of the common marmoset, but that our experimental design does not have sufficient power to bring out such evidence. However, it is also possible that the weak parietal activation in our study is not due to the characteristics of the experimental design, but to the content of the videos shown: while humans and macaques are more accustomed to the use of the upper limbs for reaching, grasping and

manipulating objects, marmosets often use their mouth if left free to choose. It is therefore possible that the use of videos depicting grasping-with-mouth actions may prove even more effective in mapping the different populations of mirror neurons in this primate species.

A limitation of the present study concerns the possible recruitment of brain areas related to eye movements: the animals in the scanner did not receive a reward and were not trained to fixate at a specific portion of the screen. As demonstrated previously by our group, the saccade circuitry in marmosets involves parts of areas 45, 8aV, 8C and 6DR (Johnston et al., 2019; Schaeffer, Gilbert, Hori, Hayrynen, et al., 2019; Selvanayagam et al., 2019) and parietal area LIP (Ghahremani et al., 2019; Schaeffer, Gilbert, Hori, Hayrynen, et al., 2019). Therefore, we cannot rule out that some of the more anterior activation in the frontal cluster may be related to potential differences in eye movement patterns. However, a previous microstimulation study from our lab also showed facial and forelimb responses in this region (Selvanayagam et al., 2019). Moreover, single neuron recordings have identified neurons involved in the generation and processing of vocalizations in these same frontal areas (45, 8Av, 6V, 6D) in marmosets (Miller et al., 2015). Single neuron electrophysiological recordings will be necessary to test whether separate neural populations perform these different functions or whether the same neurons have multiple response patterns (e.g. saccade, vocal-motor, or grasping responses).

In summary, our study provides the first evidence of an extensive action-observation network in the common marmoset. This network has important similarities with the well-characterized MNS in humans and macaques, suggesting that the common ancestor of New and Old World primates possessed a system for understanding the actions of others. The presence of a putative MNS in marmosets opens avenues to important new research perspectives in this nonhuman primate model, exploiting both invasive and non-invasive brain activity recording and manipulation techniques. Marmosets are small primates with a wide repertoire of social behaviors and live in family structures, making them particularly suitable for the study of multiple facets of primate social cognition.

Materials and Methods

All the experimental procedures here described were performed in accordance with the guidelines of the Canadian Council on Animal Care policy on the care and use of experimental animals and an animal use protocol #2021-111 approved by the Animal Care Committee of the University of Western Ontario.

Subjects and experimental setup

Four common marmosets (*Callithrix jacchus*; two females, average age: 37 ± 12 months, ranging from 30 to 55 months, average weight: 397.5 ± 45.7 g, ranging from 345 to 442 g) took part in an awake fMRI study after the surgical implantation of a MRI-compatible head restraint chamber (see Johnston et al., 2018 for details). In order to reduce stress and anxiety due to scanning and to head-fixation, all marmosets underwent a 3-week training following the acclimatization procedure prior to the experiments described in Gilbert et al. (2021). All animals scored 1 or 2 on the behavioural assessment scale described by Silva et al. (2011) after the training, reporting little or no signs of agitation and a calm behaviour.

Before MRI acquisition, the marmoset was placed in the sphinx position using the same MRI-compatible restraint system described in Schaeffer et al. (2019). After entering the animal holder, the monkey was firstly restrained using a neck and a tail plates. Taking advantage of the MRI-compatible chamber, the head of the marmoset was then fixed to the five-channel receive coil. A lubricating gel (MUKO SM1321N, Canadian Custom Packaging Company, Toronto, Ontario, Canada) was applied on the top of the chamber and on its edges in order to reduce magnetic susceptibility and artifacts. An MRI-compatible camera (model 12M-i, 60 Hz sampling rate, MRC Systems GmbH, Heidelberg, Germany) mounted on the front of the animal holder allowed the monitoring of the animal's condition and awake state by a veterinarian technician. Once in the scanner, marmosets faced a translucent plexiglass screen attached to the front of the scanner bore (~119 cm from animal's eyes) on which the visual stimuli projected by a SONY VPL-FE40 projector were reflected via a wall-mounted mirror. Maximum visual angle from the centre to the side of the screen was 6.5°. Visual stimuli were presented via PowerPoint in synchronization with MRI TTL pulses triggered by a Raspberry Pi (model 3B+, Raspberry Pi Foundation, Cambridge, UK) running a custom python script.

MRI Acquisition

All scanning sessions were carried out at the Centre for Functional and Metabolic Mapping at the University of Western Ontario, in a 9.4T, 31 cm horizontal bore magnet (Varian/Agilent) and a Bruker BioSpec Avance III console with the software package Paravision-7 (Bruker BioSpin Corp), a custom-built high-performance 15-cm diameter gradient coil with 400-mT/m maximum gradient strength (Handler et al., 2020), and a five-channel receive coil (Schaeffer, Gilbert, Hori, Gati, et al., 2019). An in-house built quadrature birdcage coil (12-cm diameter) functioned as transmit coil.

For functional imaging, gradient-echo-based, single-shot echo-planar images covering the whole brain were acquired over multiple daily sessions (TR=1500 ms; TE=15 ms; flip angle=40°; FOV=64×48 mm; matrix size=96×128; voxel size=0.5 mm isotropic; number of slices=42 [axial]; bandwidth=400 kHz. To perform anatomical registration, a T2-weighted structural image was acquired for each animal with the following parameters: TR=7000 ms; TE=52 ms; FOV=51.20 × 51.20 mm; voxel size=0.133×0.133×0.5 mm; number of slices=45 (axial); bandwidth=50 kHz.

Each session lasted approximately 50-60 minutes, including preparation of the animal and of the sequences. The number of runs acquired during each session depended on the compliance of the animal (minimum 2, maximum 6), which therefore determined the number of sessions necessary to reach the quota of runs (n=10) selected for the analyses (min number of sessions: 4, max: 7).

Task and Stimuli

Similarly to Nelissen and colleagues' studies (Nelissen et al., 2005, 2011), the visual stimuli used in this experiment consisted of movies representing reaching and grasping actions or movements of the upper limb. All videos were recorded at the non-human primate facility of the Robarts Research Institute and represented two different motor acts performed by the upper limb of a marmoset (none of the "actors" was included in the experimental sample nor was housed in the same room as the fMRI animals). Video editing was performed in Adobe Premiere Pro (Adobe, San Jose, California, USA). In the first experimental condition, hereafter called "Grasping Hand" (S1 movie), the movie represented the hand and forearm of a marmoset reaching towards and grasping a small piece of food (marshmallow, ~2 cm of diameter). In this condition, a complete goal-directed action is therefore presented in which the food is reached, grabbed and finally

transported outside the scene. In the second experimental condition, hereafter called "Empty Hand" (S2 movie), the movement of the upper limb is very similar, but in this case the action is purposeless, as no object is present in the scene. All videos lasted for 3 seconds; due to the speed of the recorded grasping movement, these clips were slightly slowed down to fill this time interval (S1 and S2 movies are examples of slowed-down actions). Twelve different videos were selected for each condition. To check the effect of the direction of action, all videos were mirrored, presenting rightward and leftward sequences within each run for each monkey. In addition, to check possible effects due simply to the perception of moving stimuli, all videos were scrambled (see S3 and S4 movies for examples of grasping and empty hand scrambled conditions respectively) by random rotation of the phase information performed with a custom MATLAB script (MATLAB, The MathWorks, Natick, MA). The use of a constant seed made it possible to preserve the aspects of motion and luminance in scrambled videos, applying the same rotation matrix to each frame of each movie. Each run included 8 stimulation blocks (two blocks for each of the four experimental conditions: grasping hand, scrambled grasping hand, empty hand and scrambled empty hand), whose order was fully randomized across runs, sessions and animals. Each block was composed of a sequence of 4 3 second videos belonging to the same experimental condition, for a duration of 12 seconds, and was preceded and followed by 18 seconds of baseline, in order to allow the washing-out of the BOLD signal between experimental blocks (total duration of a run: 258 seconds). During the baseline, a black filled circular shape (1.5 cm of diameter, 0.72°) was presented at the center of the screen. A diagram of the structure of a run can be seen in Figure 5. The compliance of the animal during each run was checked and noted online by the investigator; runs in which the animal closed its eyes for more than one stimulation block (regardless of the experimental condition) were discarded from further analyses. Animals did not receive any reward during the task.

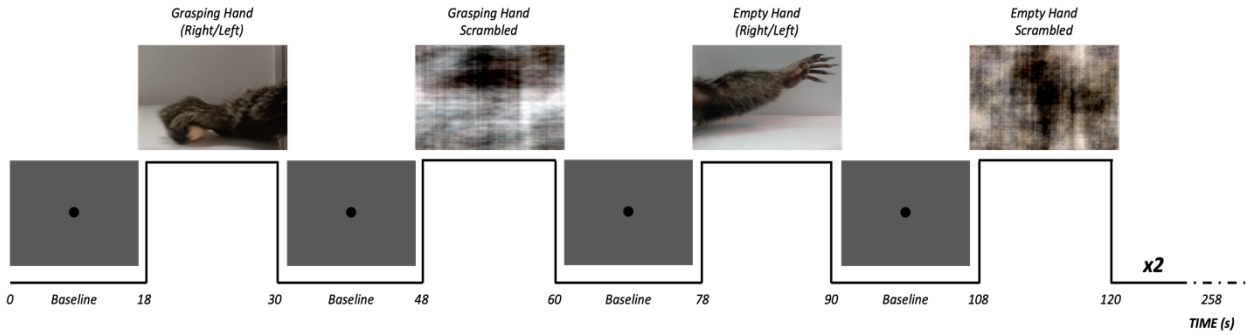

Figure 5 Experimental design for task-based fMRI. In each run, 9 baseline blocks (18 seconds long) were alternated with experimental blocks (12 seconds long) of four different conditions: Grasping Hand, Empty Hand, Grasping Hand Scrambled and Empty Hand Scrambled. Each run lasted 258 seconds globally.

Image Preprocessing

The data were preprocessed using a combination of AFNI (Cox, 1996) and FSL's functions (Smith et al., 2004). The raw functional images were first converted to the NIfTI format using dcm2niix (Li et al., 2016) and then reoriented (FSL's fslswapdim and fslorient) to correct the sphinx posture. The reoriented functional images were preprocessed through procedures for eliminating any outliers (detected via AFNI's 3dToutcount), despiking (AFNI's 3dDespike) and time shifting (AFNI's 3dTshift). The images thus obtained were registered to the base volume (extracted at the half of each run and therefore corresponding to the 86th volume) using AFNI's 3dvolreg function. Then, all volumes were smoothed (AFNI's 3dmerge, FWHM Gaussian kernel of 2mm) and bandpass-filtered (AFNI's 3dBandpass, lowest frequency of 0.1 and highest frequency of 0.01). An average functional image was calculated for each run of each animal and then registered (FSL's FLIRT function) to the respective T2-weighted image. The transformation matrix thus obtained was subsequently used to carry out the 4D time series data. T2-weighted images were manually skull-stripped (removing the olfactory bulb) and the mask obtained was applied to the functional images.

Finally, both anatomical and functional images were registered to the NIH marmoset brain atlas (Liu et al., 2018) via the nonlinear registration operated by ANTs' (Advanced Normalization Tools, Avants et al., 2011) ApplyTransforms function.

Contrasts analysis

The task timing was convolved to the BOLD response (AFNI's 3dDeconvolve) specifying the 'BLOCK' convolution and extracting a regressor for each condition (Grasping Hand, Empty Hand and the two Scrambled conditions) for each run to be used in the subsequent regression analysis. All the conditions were entered in the model, along with polynomial detrending regressors (n=5). This regression generated four T-value maps, corresponding to the four experimental conditions, per animal per run, that were registered to the NIH marmoset brain atlas (Liu et al., 2018). These maps were thus compared through paired t tests (AFNI's 3dttest++).

At the group level, the T-maps of each animal for each condition and for each run (n=10) were converted into Z value maps and compared via t-test versus 0 (AFNI's 3dttest++), in order to verify the activations of each condition with respect to the baseline. For protection against false positives, the results of these t-tests were corrected with a minimum cluster-size resulting from 10000 Monte Carlo simulations (AFNI's -Clustsim option of 3dttest++ function, considering cluster-size correction for $p<0.001$ and $\alpha=0.05$, nearest-neighbor clustering method 2, two-sided).

To investigate the neural responses induced by the perception of an "intact" biological movement versus a scrambled movement pattern, the Z value maps (n=80) of the Grasping and Empty Hand conditions of each animal were compared via t-test to those of the Scrambled Grasping Hand and Scrambled Empty Hand conditions. As before, a clustering method derived from Monte Carlo simulations was applied to the results (AFNI's 3dttest++ with Clustsim option, $p<0.001$ and $\alpha=0.05$, nearest-neighbor clustering method 2, two-sided).

Finally, the presence of areas selective for goal-directed actions was investigated by comparing the Z value maps (n=40) of the Grasping Hand and Empty Hand conditions. As in the cases described above, we compared these maps using a paired t-test, the results of which were protected from false positives thanks to the same cluster-size correction (AFNI's 3dttest++ with Clustsim option, $p<0.001$ and $\alpha=0.05$, nearest-neighbor clustering method 2, two-sided).

To compare the magnitude of the responses between conditions in brain regions classically included in the MNS of humans and macaques, six regions of interest were defined using the Paxinos parcellation of the NIH atlas (Liu et al., 2018). These ROIs include the two portions of ventral area 6 (6Va and 6Vb), area 45, the fundus of the superior temporal sulcus (FST), and the inferior parietal lobe areas PG and PFG, all bilaterally. After creating the bilateral masks of these ROIs starting from the Paxinos atlas (through AFNI's 3dcalc), the time series of each condition

were extracted (AFNI's 3dmaskave) from the regression coefficient maps of each run of each animal (obtained through AFNI's 3dDeconvolve). Once data normality was tested (Shapiro test, R's shapiro.test), the time series of each run of each animal for each condition were concatenated and compared via a paired t-test (R's t.test), keeping separate the different ROIs and correcting for multiple comparisons (R's p.adjust, FDR correction for 6 comparisons). The averages and standard errors were later calculated and plotted in RStudio (RStudio, PBC, Boston, MA).

Acknowledgements

Support was provided by the Canadian Institutes of Health Research (FRN 148365), the Canada First Research Excellence Fund to BrainsCAN, and a Discovery grant by the Natural Sciences and Engineering Research Council of Canada. We wish to thank Cheryl Vander Tuin, Whitney Froese, Hannah Pettypiece, and Miranda Bellyou for animal preparation and care, Dr. Alex Li for scanning assistance and Dr. Kevin Johnston for video footage assistance and his careful reading of this manuscript.

Competing interests

Authors do not report any conflicts of interest.

References

Arnstein, D., Cui, F., Keysers, C., Maurits, N. M., & Gazzola, V. (2011). μ-Suppression during Action Observation and Execution Correlates with BOLD in Dorsal Premotor, Inferior Parietal, and SI Cortices. *Journal of Neuroscience*, *31*(40), 14243–14249. https://doi.org/10.1523/JNEUROSCI.0963-11.2011

Avants, B. B., Tustison, N. J., Song, G., Cook, P. A., Klein, A., & Gee, J. C. (2011). A reproducible evaluation of ANTs similarity metric performance in brain image registration. *NeuroImage*, *54*(3), 2033–2044. https://doi.org/10.1016/j.neuroimage.2010.09.025

Aziz-Zadeh, L., Wilson, S. M., Rizzolatti, G., & Iacoboni, M. (2006). Congruent Embodied Representations for Visually Presented Actions and Linguistic Phrases Describing Actions. *Current Biology*, *16*(18), 1818–1823. https://doi.org/10.1016/j.cub.2006.07.060

Bekkali, S., Youssef, G. J., Donaldson, P. H., Albein-Urios, N., Hyde, C., & Enticott, P. G. (2021). Is the Putative Mirror Neuron System Associated with Empathy? A Systematic Review and Meta-Analysis. *Neuropsychology Review*, *31*(1), 14–57. https://doi.org/10.1007/s11065-020-09452-6

Buccino, G., Binkofski, F., & Riggio, L. (2004). The mirror neuron system and action recognition. *Brain and Language*, *89*(2), 370–376. https://doi.org/10.1016/S0093-934X(03)00356-0

Burman, K. J., Bakola, S., Richardson, K. E., Yu, H.-H., Reser, D. H., & Rosa, M. G. P. (2015). Cortical and thalamic projections to cytoarchitectural areas 6Va and 8C of the marmoset monkey: Connectionally distinct subdivisions of the lateral premotor cortex. *Journal of Comparative Neurology*, *523*(8), 1222–1247. https://doi.org/10.1002/cne.23734

Casile, A. (2013). Mirror neurons (and beyond) in the macaque brain: An overview of 20 years of research. *Neuroscience Letters*, *540*, 3–14. https://doi.org/10.1016/j.neulet.2012.11.003

Chong, T. T.-J., Cunnington, R., Williams, M. A., Kanwisher, N., & Mattingley, J. B. (2008). FMRI Adaptation Reveals Mirror Neurons in Human Inferior Parietal Cortex. *Current Biology*, *18*(20), 1576–1580. https://doi.org/10.1016/j.cub.2008.08.068

Cisek, P., & Kalaska, J. F. (2004). Neural correlates of mental rehearsal in dorsal premotor cortex. *Nature*, *431*(7011), 993–996. https://doi.org/10.1038/nature03005

Cléry, J. C., Hori, Y., Schaeffer, D. J., Menon, R. S., & Everling, S. (2021). Neural network of social interaction observation in marmosets. *ELife*, *10*, e65012. https://doi.org/10.7554/eLife.65012

Cox, R. W. (1996). AFNI: Software for Analysis and Visualization of Functional Magnetic Resonance Neuroimages. *Computers and Biomedical Research*, *29*(3), 162–173. https://doi.org/10.1006/cbmr.1996.0014

di Pellegrino, G., Fadiga, L., Fogassi, L., Gallese, V., & Rizzolatti, G. (1992). Understanding motor events: A neurophysiological study. *Experimental Brain Research*, *91*(1), 176–180. https://doi.org/10.1007/BF00230027

Dushanova, J., & Donoghue, J. (2010). Neurons in primary motor cortex engaged during action observation. *European Journal of Neuroscience*, *31*(2), 386–398. https://doi.org/10.1111/j.1460-9568.2009.07067.x

Fadiga, L., Craighero, L., & Olivier, E. (2005). Human motor cortex excitability during the perception of others' action. *Current Opinion in Neurobiology*, *15*(2), 213–218. https://doi.org/10.1016/j.conb.2005.03.013

Farina, E., Borgnis, F., & Pozzo, T. (2020). Mirror neurons and their relationship with neurodegenerative disorders. *Journal of Neuroscience Research*, *98*(6), 1070–1094. https://doi.org/10.1002/jnr.24579

Ferrari, P. F., Gallese, V., Rizzolatti, G., & Fogassi, L. (2003). Mirror neurons responding to the observation of ingestive and communicative mouth actions in the monkey ventral premotor cortex. *European Journal of Neuroscience*, *17*(8), 1703–1714. https://doi.org/10.1046/j.1460-9568.2003.02601.x

Ferri, S., Peeters, R., Nelissen, K., Vanduffel, W., Rizzolatti, G., & Orban, G. A. (2015). A human homologue of monkey F5c. *NeuroImage*, *111*, 251–266. https://doi.org/10.1016/j.neuroimage.2015.02.033

Fogassi, L., Ferrari, P. F., Gesierich, B., Rozzi, S., Chersi, F., & Rizzolatti, G. (2005). Parietal Lobe: From Action Organization to Intention Understanding. *Science*, *308*(5722), 662–667. https://doi.org/10.1126/science.1106138

Fogassi, L., & Luppino, G. (2005). Motor functions of the parietal lobe. *Current Opinion in Neurobiology*, *15*(6), 626–631. https://doi.org/10.1016/j.conb.2005.10.015

Gallese, V., Fadiga, L., Fogassi, L., & Rizzolatti, G. (1996). Action recognition in the premotor cortex. *Brain*, *119*(2), 593–609. https://doi.org/10.1093/brain/119.2.593

Gallese, V., Fogassi, L., Fadiga, L., & Rizzolatti, G. (2002). Action representation and the inferior parietal lobule. In *Attention and performance XIX* (W. Prinz&B. Hommel, pp. 247–266). Oxford University Press.

Ghahremani, M., Hutchison, R. M., Menon, R. S., & Everling, S. (2017). Frontoparietal Functional Connectivity in the Common Marmoset. *Cerebral Cortex*, *27*(8), 3890–3905. https://doi.org/10.1093/cercor/bhw198

Ghahremani, M., Johnston, K. D., Ma, L., Hayrynen, L. K., & Everling, S. (2019). Electrical microstimulation evokes saccades in posterior parietal cortex of common marmosets. *Journal of Neurophysiology*, *122*(4), 1765–1776. https://doi.org/10.1152/jn.00417.2019

Gilbert, K. M., Cléry, J. C., Gati, J. S., Hori, Y., Johnston, K. D., Mashkovtsev, A., Selvanayagam, J., Zeman, P., Menon, R. S., Schaeffer, D. J., & Everling, S. (2021). Simultaneous functional MRI of two awake marmosets. *Nature Communications*, *12*, 6608. https://doi.org/10.1038/s41467-021-26976-4

Grèzes, J., Armony, J. L., Rowe, J., & Passingham, R. E. (2003). Activations related to "mirror" and "canonical" neurones in the human brain: An fMRI study. *NeuroImage*, *18*(4), 928–937. https://doi.org/10.1016/S1053-8119(03)00042-9

Handler, W. B., Bindseil, G., Chaddock, R., Dalrymple, B., Gati, J. S., Gilbert, K. M., Harris, C. T., Klassen, M. L., Peterson, J., Sas, F. V., & Chronik, B. A. (2020). Design and construction of a gradient coil for high resolution marmoset imaging. *Biomedical Physics & Engineering Express*, *6*(4), 045022. https://doi.org/10.1088/2057-1976/ab8d97

Hori, Y., Cléry, J. C., Selvanayagam, J., Schaeffer, D. J., Johnston, K. D., Menon, R. S., & Everling, S. (2021). Interspecies activation correlations reveal functional correspondences between marmoset and human brain areas. *Proceedings of the National Academy of Sciences*, *118*(37), e2110980118. https://doi.org/10.1073/pnas.2110980118

Hung, C.-C., Yen, C. C., Ciuchta, J. L., Papoti, D., Bock, N. A., Leopold, D. A., & Silva, A. C. (2015). Functional Mapping of Face-Selective Regions in the Extrastriate Visual Cortex of the Marmoset. *Journal of Neuroscience*, *35*(3), 1160–1172. https://doi.org/10.1523/JNEUROSCI.2659-14.2015

Iacoboni, M., Woods, R. P., Brass, M., Bekkering, H., Mazziotta, J. C., & Rizzolatti, G. (1999). Cortical Mechanisms of Human Imitation. *Science*, *286*(5449), 2526–2528. https://doi.org/10.1126/science.286.5449.2526

Johnston, K. D., Barker, K., Schaeffer, L., Schaeffer, D., & Everling, S. (2018). Methods for chair restraint and training of the common marmoset on oculomotor tasks. *Journal of Neurophysiology*, *119*(5), 1636–1646. https://doi.org/10.1152/jn.00866.2017

Johnston, K. D., Ma, L., Schaeffer, L., & Everling, S. (2019). Alpha Oscillations Modulate Preparatory Activity in Marmoset Area 8Ad. *The Journal of Neuroscience*, *39*(10), 1855–1866. https://doi.org/10.1523/JNEUROSCI.2703-18.2019

Kilner, J. M., Neal, A., Weiskopf, N., Friston, K. J., & Frith, C. D. (2009). Evidence of Mirror Neurons in Human Inferior Frontal Gyrus. *Journal of Neuroscience*, *29*(32), 10153–10159. https://doi.org/10.1523/JNEUROSCI.2668-09.2009

Li, X., Morgan, P. S., Ashburner, J., Smith, J., & Rorden, C. (2016). The first step for neuroimaging data analysis: DICOM to NIfTI conversion. *Journal of Neuroscience Methods*, *264*, 47–56. https://doi.org/10.1016/j.jneumeth.2016.03.001

Liu, C., Ye, F. Q., Yen, C. C.-C., Newman, J. D., Glen, D., Leopold, D. A., & Silva, A. C. (2018). A digital 3D atlas of the marmoset brain based on multi-modal MRI. *NeuroImage*, *169*, 106–116. https://doi.org/10.1016/j.neuroimage.2017.12.004

Matelli, M., Camarda, R., Glickstein, M., & Rizzolatti, G. (1986). Afferent and efferent projections of the inferior area 6 in the macaque monkey. *Journal of Comparative Neurology*, *251*(3), 281–298. https://doi.org/10.1002/cne.902510302

Miller, C. T., Thomas, A. W., Nummela, S. U., & de la Mothe, L. A. (2015). Responses of primate frontal cortex neurons during natural vocal communication. *Journal of Neurophysiology*, *114*(2), 1158–1171. https://doi.org/10.1152/jn.01003.2014

Molenberghs, P., Cunnington, R., & Mattingley, J. B. (2012). Brain regions with mirror properties: A meta-analysis of 125 human fMRI studies. *Neuroscience & Biobehavioral Reviews*, *36*(1), 341–349. https://doi.org/10.1016/j.neubiorev.2011.07.004

Mukamel, R., Ekstrom, A. D., Kaplan, J., Iacoboni, M., & Fried, I. (2010). Single-Neuron Responses in Humans during Execution and Observation of Actions. *Current Biology*, *20*(8), 750–756. https://doi.org/10.1016/j.cub.2010.02.045

Nelissen, K., Borra, E., Gerbella, M., Rozzi, S., Luppino, G., Vanduffel, W., Rizzolatti, G., & Orban, G. A. (2011). Action Observation Circuits in the Macaque Monkey Cortex. *Journal of Neuroscience*, *31*(10), 3743–3756. https://doi.org/10.1523/JNEUROSCI.4803-10.2011

Nelissen, K., Luppino, G., Vanduffel, W., Rizzolatti, G., & Orban, G. A. (2005). Observing Others: Multiple Action Representation in the Frontal Lobe. *Science*, *310*(5746), 332–336. https://doi.org/10.1126/science.1115593

Nogueira, N. G. de H. M., Parma, J. O., Leão, S. E. S. de A., Sales, I. de S., Macedo, L. C., Galvão, A. C. D. R., de Oliveira, D. C., Murça, T. M., Fernandes, L. A., Junqueira, C., Lage, G. M., & Ferreira, B. de P. (2021). Mirror therapy in upper limb motor recovery and activities of daily living, and its neural correlates in stroke individuals: A systematic review and meta-analysis. *Brain Research Bulletin*, *177*, 217–238. https://doi.org/10.1016/j.brainresbull.2021.10.003

Okano, H. (2021). Current Status of and Perspectives on the Application of Marmosets in Neurobiology. *Annual Review of Neuroscience*, *44*(1), 27–48. https://doi.org/10.1146/annurev-neuro-030520-101844

Paz, L. V., Viola, T. W., Milanesi, B. B., Sulzbach, J. H., Mestriner, R. G., Wieck, A., & Xavier, L. L. (2022). Contagious depression: Automatic mimicry and the mirror neuron system - A review. *Neuroscience & Biobehavioral Reviews*, *134*, 104509. https://doi.org/10.1016/j.neubiorev.2021.12.032

Perrett, D. I., Harries, M. H., Bevan, R., Thomas, S., Benson, P. J., Mistlin, A. J., Chttty, A. J., Hietanen, J. K., & Ortega, J. E. (1989). Frameworks of analysis for the neural representation of animate objects and actions. *Journal of Experimental Biology*, *146*(1), 87–113.

Petrides, M., & Pandya, D. N. (1984). Projections to the frontal cortex from the posterior parietal region in the rhesus monkey. *Journal of Comparative Neurology*, *228*(1), 105–116. https://doi.org/10.1002/cne.902280110

Ramsey, R., Kaplan, D. M., & Cross, E. S. (2021). Watch and Learn: The Cognitive Neuroscience of Learning from Others' Actions. *Trends in Neurosciences*, *44*(6), 478–491. https://doi.org/10.1016/j.tins.2021.01.007

Rizzolatti, G., & Craighero, L. (2004). The Mirror-Neuron System. *Annual Review of Neuroscience*, *27*(1), 169–192. https://doi.org/10.1146/annurev.neuro.27.070203.144230

Rizzolatti, G., Fabbri-Destro, M., Nuara, A., Gatti, R., & Avanzini, P. (2021). The role of mirror mechanism in the recovery, maintenance, and acquisition of motor abilities. *Neuroscience and Biobehavioral Reviews*, *127*, 404–423. https://doi.org/10.1016/j.neubiorev.2021.04.024

Rizzolatti, G., Fadiga, L., Gallese, V., & Fogassi, L. (1996). Premotor cortex and the recognition of motor actions. *Cognitive Brain Research*, 131–141.

Rizzolatti, G., Fogassi, L., & Gallese, V. (2001). Neurophysiological mechanisms underlying the understanding and imitation of action. *Nature Reviews Neuroscience*, *2*(9), 661–670. https://doi.org/10.1038/35090060

Rozzi, S., Ferrari, P. F., Bonini, L., Rizzolatti, G., & Fogassi, L. (2008). Functional organization of inferior parietal lobule convexity in the macaque monkey: Electrophysiological characterization of motor, sensory and mirror responses and their correlation with cytoarchitectonic areas. *European Journal of Neuroscience*, *28*(8), 1569–1588. https://doi.org/10.1111/j.1460-9568.2008.06395.x

Saxe, R., Xiao, D.-K., Kovacs, G., Perrett, D. I., & Kanwisher, N. (2004). A region of right posterior superior temporal sulcus responds to observed intentional actions. *Neuropsychologia*, *42*(11), 1435–1446. https://doi.org/10.1016/j.neuropsychologia.2004.04.015

Schaeffer, D. J., Gilbert, K. M., Hori, Y., Gati, J. S., Menon, R. S., & Everling, S. (2019). Integrated radiofrequency array and animal holder design for minimizing head motion during awake marmoset functional magnetic resonance imaging. *NeuroImage*, *193*, 126–138. https://doi.org/10.1016/j.neuroimage.2019.03.023

Schaeffer, D. J., Gilbert, K. M., Hori, Y., Hayrynen, L. K., Johnston, K. D., Gati, J. S., Menon, R. S., & Everling, S. (2019). Task-based fMRI of a free-viewing visuo-saccadic network in the marmoset monkey. *NeuroImage*, *202*, 116147. https://doi.org/10.1016/j.neuroimage.2019.116147

Schaeffer, D. J., Selvanayagam, J., Johnston, K. D., Menon, R. S., Freiwald, W. A., & Everling, S. (2020). Face selective patches in marmoset frontal cortex. *Nature Communications*, *11*(1), 4856. https://doi.org/10.1038/s41467-020-18692-2

Seltzer, B., & Pandya, D. N. (1989). Frontal lobe connections of the superior temporal sulcus in the rhesus monkey. *Journal of Comparative Neurology*, *281*(1), 97–113. https://doi.org/10.1002/cne.902810108

Selvanayagam, J., Johnston, K. D., Schaeffer, D. J., Hayrynen, L. K., & Everling, S. (2019). Functional Localization of the Frontal Eye Fields in the Common Marmoset Using Microstimulation. *The Journal of Neuroscience*, *39*(46), 9197–9206. https://doi.org/10.1523/JNEUROSCI.1786-19.2019

Silva, A. C., Liu, J. V., Hirano, Y., Leoni, R. F., Merkle, H., Mackel, J. B., Zhang, X. F., Nascimento, G. C., & Stefanovic, B. (2011). Longitudinal functional magnetic resonance imaging in animal models. In M. Modo & J. W. M. Bulte (Eds.), *Magnetic resonance neuroimaging: Methods and protocols* (pp. 281–302). Humana Press.

Sliwa, J., & Freiwald, W. A. (2017). A dedicated network for social interaction processing in the primate brain. *Science*, *356*(6339), 745–749. https://doi.org/10.1126/science.aam6383

Smith, S. M., Jenkinson, M., Woolrich, M. W., Beckmann, C. F., Behrens, T. E. J., Johansen-Berg, H., Bannister, P. R., De Luca, M., Drobnjak, I., Flitney, D. E., Niazy, R. K., Saunders, J., Vickers, J., Zhang, Y., De Stefano, N., Brady, J. M., & Matthews, P. M. (2004). Advances in functional and structural MR image analysis and implementation as FSL. *NeuroImage*, *23*, S208–S219. https://doi.org/10.1016/j.neuroimage.2004.07.051

Suzuki, W., Banno, T., Miyakawa, N., Abe, H., Goda, N., & Ichinohe, N. (2015). Mirror Neurons in a New World Monkey, Common Marmoset. *Frontiers in Neuroscience*, *9*. https://www.frontiersin.org/article/10.3389/fnins.2015.00459

Theodoni, P., Majka, P., Reser, D. H., Wójcik, D. K., Rosa, M. G. P., & Wang, X.-J. (2022). Structural Attributes and Principles of the Neocortical Connectome in the Marmoset Monkey. *Cerebral Cortex*, *32*(1), 15–28. https://doi.org/10.1093/cercor/bhab191

Tkach, D., Reimer, J., & Hatsopoulos, N. G. (2007). Congruent Activity during Action and Action Observation in Motor Cortex. *Journal of Neuroscience*, *27*(48), 13241–13250. https://doi.org/10.1523/JNEUROSCI.2895-07.2007

Umiltà, M. A., Kohler, E., Gallese, V., Fogassi, L., Fadiga, L., Keysers, C., & Rizzolatti, G. (2001). I Know What You Are Doing: A Neurophysiological Study. *Neuron*, *31*(1), 155–165. https://doi.org/10.1016/S0896-6273(01)00337-3

Yates, L., & Hobson, H. (2020). Continuing to look in the mirror: A review of neuroscientific evidence for the broken mirror hypothesis, EP-M model and STORM model of autism spectrum conditions. *Autism: The International Journal of Research and Practice*, *24*(8), 1945–1959. https://doi.org/10.1177/1362361320936945

Supplementary materials

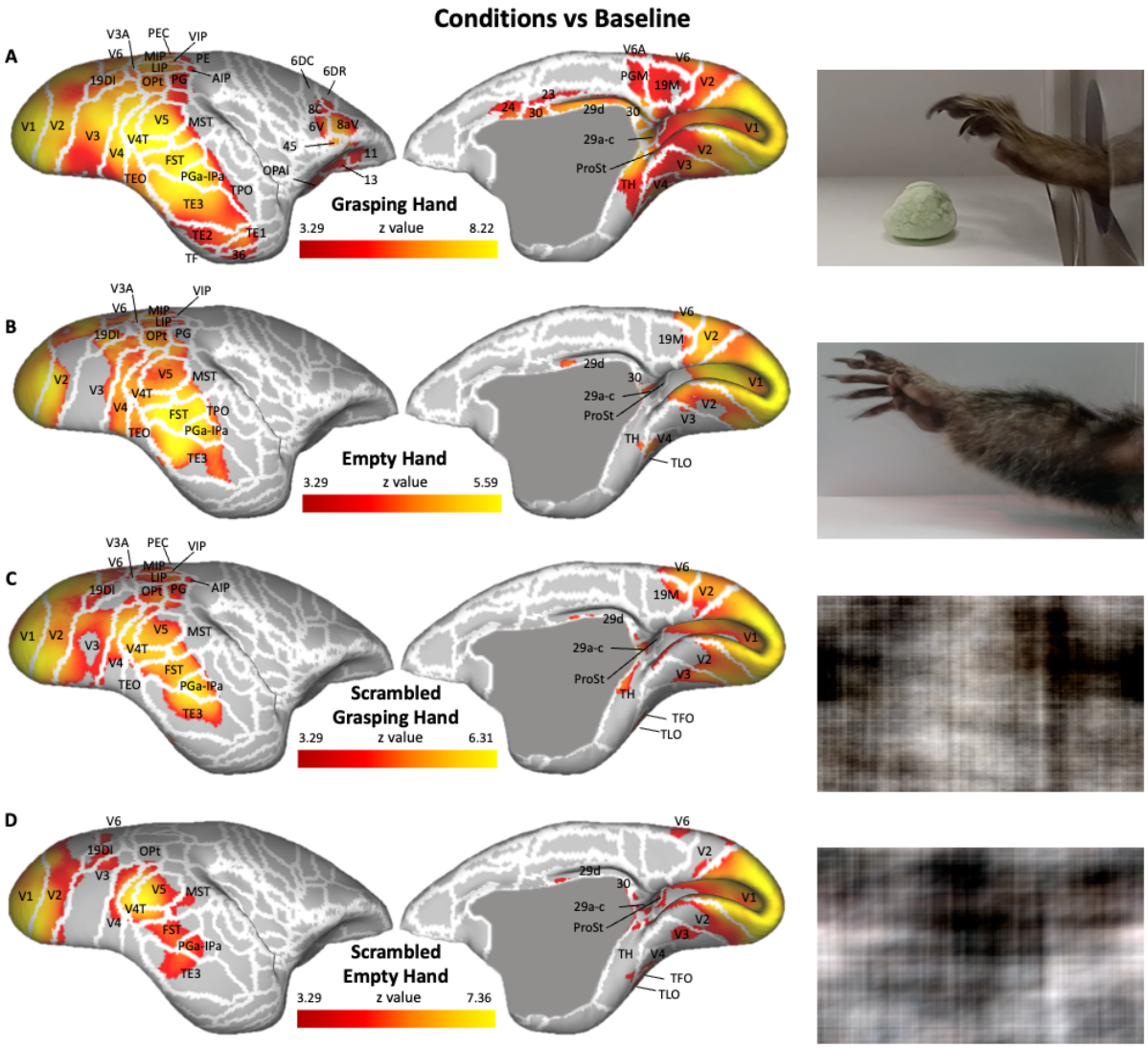

Figure S1. Functional maps of the contrasts between Grasping Hand (A), Empty Hand (B), Scrambled Grasping Hand (C) and Scrambled Empty Hand (D) conditions and the baseline. Maps are displayed on the right fiducial brain surface (lateral view on the left, medial view on the right). White lines delineate the cerebral areas included in the Paxinos parcellation of the NIH marmoset brain atlas (Liu et al., 2018). The responses here reported have intensity higher than z = 3.29 (corresponding to $p<0.001$, AFNI's 3dttest++) and survived the cluster-size correction (10000 Monte-Carlo simulations, with $\alpha=0.05$).